

# Analysis of Leakage Inductances in Shunt Reactors: Application to High Voltage Transmission Lines

Tu Pham Minh

School of Electrical and Electronic Engineering  
Hanoi University of Science and Technology  
Hanoi, Vietnam  
tu.phamminh@hust.edu.vn

Hung Bui Duc

School of Electrical and Electronic Engineering  
Hanoi University of Science and Technology  
Hanoi, Vietnam  
hung.buiduc@hust.edu.vn

Vuong Dang Quoc

School of Electrical and Electronic Engineering  
Hanoi University of Science and Technology  
Hanoi, Vietnam  
vuong.dangquoc@hust.edu.vn

Received: 12 February 2022 | Revised: 1 March 2022 | Accepted: 16 March 2022

**Abstract**—Inductance is one of the main parameters directly related to the reactive powers of Shunt Reactors (SRs) in electrical systems. Thus, the definition and computation of leakage inductances and the ratio of leakage to total inductances play an extremely important role in the design and manufacturing of SRs. In this study, a finite element approach was developed to compute leakage and total inductances and define a relationship between them with different SR powers and high voltage levels. The expanded method is presented with the magnetic vector potential formulations.

**Keywords**—shunt reactor; leakage inductance; magnetic vector potential formulation; finite element method

## I. INTRODUCTION

In long-distance high voltage transmission lines, capacitances occur between the phase voltage and earth or between phase voltages, leading to large reactive power in the electrical system [1-3]. In general, when a system operates on a full load, the reactive power is absorbed by the inductance load and lines. On the other hand, if the system works on low or no load, the voltage along lines increases, leading to overload voltage at the end of the line and affecting directly the electrical devices. Therefore, to overcome these drawbacks and maintain voltage stability in the electrical system, a Shunt Reactor (SR) is proposed to absorb the generated reactive powers [1-9]. The total inductance values, consisting of fringing and leakage inductances, are needed to compute and analyze the reactive power capacity of an SR. Fringing inductances have been recently proposed in [4, 10].

In this study, a finite element approach was developed with magnetic vector potential formulations to calculate and analyze the leakage inductances of an SR. Based on the obtained results, a relation of the shape factors of an SR, between inductance leakages and total inductance, was proposed to help

researchers and designers to select suitable leakage inductances for computing and designing.

## II. MAGNETODYNAMIC PROBLEMS

### A. Maxwell's Equations

A canonical magneto-dynamic problem is defined in a domain  $\Omega$ , with boundary:

$$\partial\Omega = \Gamma = \Gamma_h \cup \Gamma_e$$

Maxwell's equations, considered in the frequency domain and behavior laws, are written in the Euclidean space  $\mathbb{R}^3$  as [11-12]:

$$\text{curl } H = J_s \quad (1-a)$$

$$\text{curl } E = -j\omega B \quad (1-b)$$

$$\text{div } B = 0 \quad (1-c)$$

$$B = \mu H \quad (2-a)$$

$$J = \sigma E \quad (2-b)$$

where  $H$  is the magnetic field (A/m),  $B$  is the magnetic flux density (T),  $E$  is the electric field (V/m),  $J_s$  is the current density (A/m<sup>2</sup>), and  $\mu$  and  $\sigma$  are the relative permeability and electric conductivity (S/m), respectively. The Boundary Conditions (BCs) defined on  $\Gamma$  are expressed as [11-12]:

$$n \times H|_{\Gamma_h} = 0 \quad (3-a)$$

$$n \cdot B|_{\Gamma_e} = 0 \quad (3-b)$$

where  $n$  is the unit normal exterior to  $\Omega$ , with  $\Omega = \Omega_c \cup \Omega_c^c$ . The domains  $\Omega_c$  and  $\Omega_c^c$  are the conducting and non-conducting regions, respectively. The equations (1-a) and (1-b) were solved with BCs taking into account the tangential component of  $H$  in (3-a) and the normal component of  $B$  in (3-b).

The fields  $H$ ,  $B$ ,  $E$ , and  $J$  are defined to satisfy Tonti's diagram [12]. This means that  $H \in F_h(\text{curl}; \Omega)$ ,  $E \in F_e(\text{curl}; \Omega)$ ,  $J \in H(\text{div}; \Omega)$ , and  $B \in F_b(\text{div}; \Omega)$ , where  $F_h(\text{curl}; \Omega)$  and  $F_e(\text{div}; \Omega)$  are function spaces containing BCs and the fields defined on  $\Gamma_h$  and  $\Gamma_e$  of the studied domain  $\Omega$ .

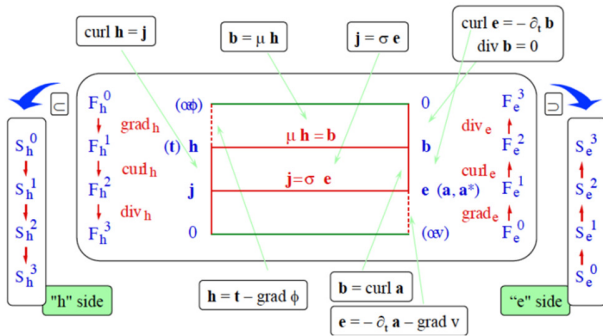


Fig. 1. Tonti's diagram [12].

The field  $B$  in (1-c) is derived from a vector potential  $A$  such that:

$$B = \text{curl } A \quad (4)$$

Combining (4) with (1-b), leads to the definition of an electric scalar potential  $v$  such that:

$$E = -\partial_t A - \text{grad } v \quad (5)$$

**B. Magnetic Vector Potential Weak Formulations**

Based on the weak form of Ampere's law (1-a), the weak formulation of magnetic problems is written as [11-13]:

$$\frac{1}{\mu} \oint_{\Omega} (\text{curl } A \cdot \text{curl } t) d\Omega - \sigma \oint_{\Omega_c} (\partial_t A \cdot \text{curl } t) d\Omega_c + \sigma \oint_{\Omega_c} (\text{grad } v \cdot \text{curl } t) d\Omega_c + \int_{\Gamma} (n \times H) \cdot t d\Gamma = \oint_{\Omega_s} (J_s \cdot t) d\Omega_s, \forall t \in F_e^0(\text{curl}, \Omega) \quad (6)$$

where  $F_e^0(\text{curl}, \Omega)$  is a function space defined on  $\Omega$  and containing the basis functions for  $A$  and the test function  $t$ . The surface integral term  $\langle n \times H, t \rangle_{\Gamma_h}$  on  $\Gamma_h$  in (6) accounts for the natural BCs and can be given in (3a-b). The energy density ( $w_t$ ) is defined via the post-processing, i.e:

$$w_m = \frac{1}{2} \oint_{\Omega} H \cdot B d\Omega \quad (7)$$

Finally, the inductance value ( $L$ ) is computed via (7), being:

$$L = \frac{2w_m}{I^2} \quad (8)$$

**III. ANALYSIS OF THE PRACTICAL TEST**

The practical test problem was a single-phase SR of 35MVar (500/ $\sqrt{3}$ kV and 50Hz). A simple model of this single-phase SR is presented in Figure 2. The typical parameters are given in Table I [4]. The percentage of the leakage inductance to the total can be defined as:

$$k_l \% = \frac{L_{leakage}}{L_{total}} \times 100 \quad (9)$$

where  $L_{leakage}$  (H) and  $L_{total}$  (H) are the leakage and total inductances of the SR respectively. The distribution of the magnetic vector potentials due to the current following in the winding is presented in Figure 3. The percentage ratio of  $L_{leakage}$  to  $L_{total}$  ( $k_l$  %) for different reactive powers and voltage levels is shown in Figure 4.

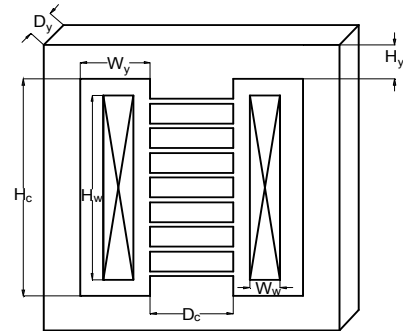


Fig. 2. Model of a single-phase shunt reactor.

TABLE I. TYPICAL PARAMETERS OF THE SR

Parameters	Notations	Values
Reactive power	Q (MVar)	35
Rated voltage	U (kV)	500/ $\sqrt{3}$
Rated current	I (A)	121.24
Total inductance	L (H)	7.5788
Core dimension	$D_c$ (mm)	701
Height of core	$H_c$ (mm)	1793
Total air gap length	$l_g$ (mm)	386
Turn number	N (turn)	2018

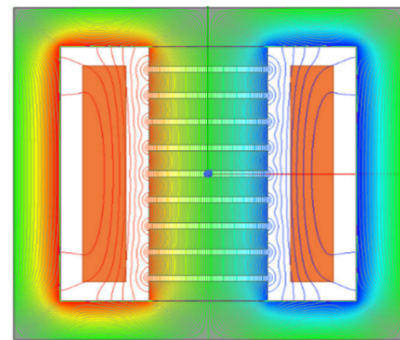


Fig. 3. Distribution of magnetic vector potentials.

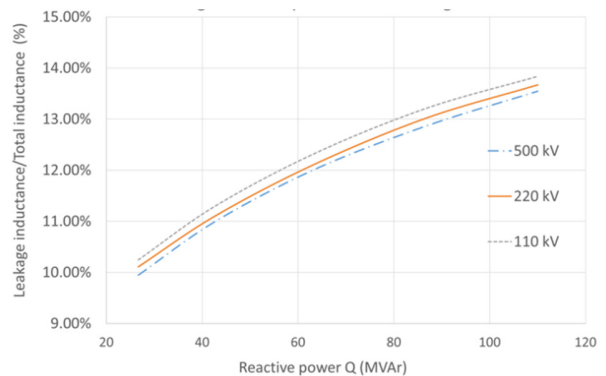


Fig. 4. Ratio of  $L_{leakage}$  to  $L_{total}$  ( $k_l$  %) for different voltage levels.

As can be noted, at the same voltage level, when the reactive power increases, the ratio of leakage inductance to total inductance also increases. From the obtained results, a polynomial function of the leakage inductance, power, and voltage, is expressed via the Lagrange interpolation method [14]. According to the Lagrange interpolation theory, it is possible to determine a polynomial function  $P(x)$  of degree less than or equal to  $n$  satisfying the conditions  $P(x_i) = y_i$ , for  $i = 1 \dots n+1$ . The general formula is written as:

$$P(x) = \sum_{i=1}^{n+1} y_i \prod_{j \neq i} \frac{x-x_j}{x_i-x_j} \quad (10)$$

where  $x_i$  can be considered as the voltage ( $U$ ), power ( $Q$ ), and  $y_i$  is the ratio of the total value of leakage flux. Based on (10), the polynomial leakage inductance according to power and voltage is defined as:

$$\%L_{leakage} = f(Q, U) = (-9.913 \times 10^{-10}U^2 + 6.116 \times 10^{-7}U - 3.451 \times 10^{-4})Q^2 + (1.329 \times 10^{-7}U^2 - 8.83 \times 10^{-5}U + 9.037 \times 10^{-2})Q - (9.008 \times 10^{-7}U^2 + 3.002 \times 10^{-5}U - 8.289) \quad (11)$$

where  $Q$  (MVar) is the reactive power and  $U$  (kV) is the voltage. Polynomial (10) allows determining the percentage of leakage inductance at different reactive powers and voltage values. In addition, leakage inductance depends significantly on the winding factor ( $k_w$ ) in the magnetic core's window. It is shown that  $k_w$  is the basis to determine the overall shape of the magnetic core. For each value of different reactive power and voltage, the value of  $L_{leakage}$  is computed with the different value of  $k_w$  ( $k_w = 4 \div 12$ ) for a change step of 0.2, as shown in Figure 5.

A polynomial function of the leakage inductance value at the high voltage level of 110 kV is defined as:

$$k_{l(110kV)}\% = f(k_w, Q) = (-4.753 \times 10^{-6}Q^2 + 10.61 \times 10^{-4}Q + 0.1136)k_w^2 + (1.127 \times 10^{-4}Q^2 - 2.627 \times 10^{-2}Q - 2.704)k_w + (-9.091 \times 10^{-4}Q^2 + 0.2223 \times 10^{-2}Q + 20.85) \quad (12)$$

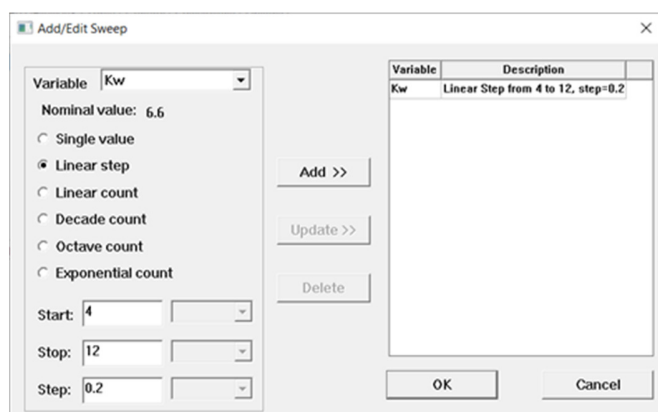


Fig. 5. Calculation of the leakage inductance with the change of winding factor.

In the same way, the leakage inductance value at the high voltage level of 220kV is expressed as:

$$k_{l(220kV)}\% = f(k_w, Q) = (-5.069 \times 10^{-6}Q^2 + 10.3 \times 10^{-4}Q + 0.1068)k_w^2 + (1.154 \times 10^{-4}Q^2 - 2.517 \times 10^{-2}Q - 2.567)k_w + (-8.932 \times 10^{-4}Q^2 + 0.2135 \times 10^{-2}Q + 20.15) \quad (13)$$

For the extra high voltage level of 500kV, the leakage inductance is computed as:

$$k_{l(500kV)}\% = f(k_w, Q) = (-4.823 \times 10^{-6}Q^2 + 9.908 \times 10^{-4}Q + 0.1046)k_w^2 + (1.11 \times 10^{-4}Q^2 - 2.432 \times 10^{-2}Q - 2.521)k_w + (-8.535 \times 10^{-4}Q^2 + 0.2063 \times 10^{-2}Q + 19.94) \quad (14)$$

Based on the polynomial functions given in (12), (13), and (14), the percentage of leakage inductance to total inductance  $k_l$  (%) according to  $k_w$  at different reactive powers and voltage levels is shown in Figures 6-8.

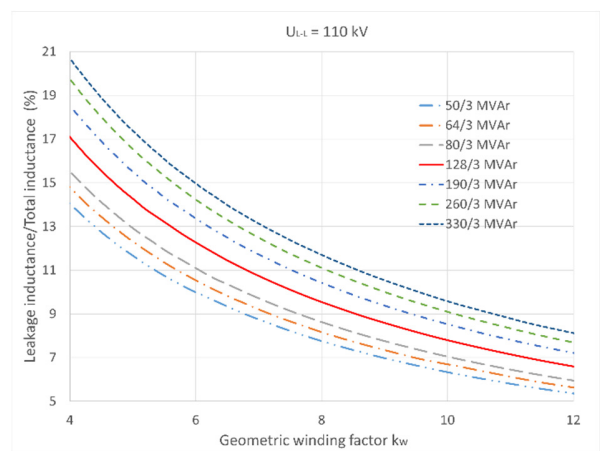


Fig. 6. The value of  $k_l$ (%) flowing to  $k_w$  with different powers at 110kV.

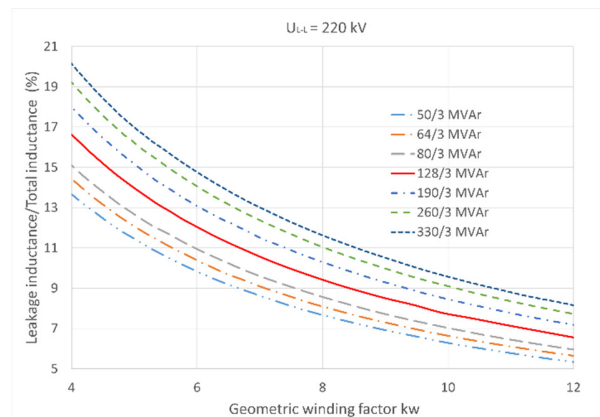


Fig. 7. The value of  $k_l$ (%) flowing to  $k_w$  with different powers at 220kV.

Based on the results shown in Figures 6-8 and the polynomial functions of the leakage inductance according to the winding factor at different reactive powers and voltage levels, this method can be a basis for researchers, designers, and manufacturers to choose and look up leakage inductance values when calculating the design, and thus reduce the number of the needed virtual object models.

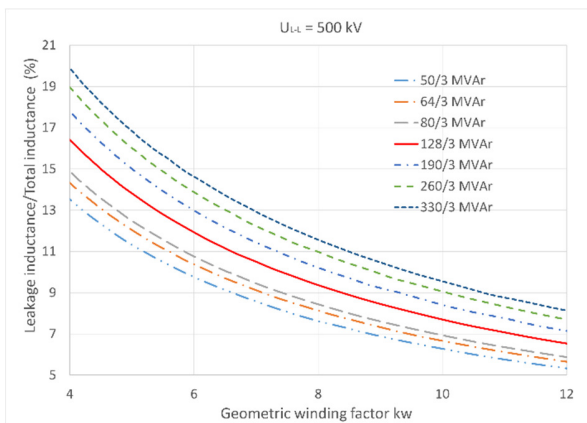


Fig. 8. The value of  $k_l$ (%) flowing to  $k_w$  with different powers at 500kV.

#### IV. CONCLUSION

A finite element approach was developed with the magnetic vector potential formulations. Based on the development of the formulation, the leakage and total inductance values according to the winding factor were defined at different reactive powers and voltage levels of 110kV, 220kV, and 500kV. The proposed method and the obtained results could help designers and manufacturers to make a suitable selection of the leakage inductance during the design or manufacturing of the SRs. The obtained results also show that there is a very good agreement on standardizing the type of leakage inductances in the SR.

#### ACKNOWLEDGMENT

This study was funded by the Hanoi University of Science and Technology (HUST) under grant number T2021-PC-006. The authors also gratefully acknowledge the Quy Nhon University, which provided favorable conditions for the use of the copyright-supported Ansys Electronics Desktop V19.R1.

#### REFERENCES

- [1] Z. Norouzian, "Shunt Reactors: Optimizing Transmission Voltage System," ABB Transformers and Reactors, Oct. 2016.
- [2] Z. Lubošny, J. Klucznik, and K. Dobrzyński, "The Issues of Reactive Power Compensation in High-voltage Transmission Lines," *Acta Energetica*, no. 23, pp. 102–108, Jun. 2015, <https://doi.org/10.12736/issn.2300-3022.2015210>.
- [3] A. S. Nunes, P. Kuo-Peng, and M. G. Vanti, "Air Core Reactor Analysis Based on RNM Method," presented at the Compumag 2013 - 19th International Conference on the Computation of Electromagnetic Fields, Budapest, Hungary, Jul. 2013, Art. no. 3.
- [4] T. P. Minh *et al.*, "Finite Element Modeling of Shunt Reactors Used in High Voltage Power Systems," *Engineering, Technology & Applied Science Research*, vol. 11, no. 4, pp. 7411–7416, Aug. 2021, <https://doi.org/10.48084/etasr.4271>.
- [5] T. Pham Minh, H. Bui Duc, T. Tran Van, D. Dang Chi, and V. Dang Quoc, "Investigating Effects of Distance Air-Gaps on Iron-Core Shunt Reactors," in *Advances in Engineering Research and Application*, Cham, 2022, pp. 545–557, [https://doi.org/10.1007/978-3-030-92574-1\\_57](https://doi.org/10.1007/978-3-030-92574-1_57).
- [6] H. Amreiz, A. Janbey, and M. Darwish, "Emulation of Series and Shunt Reactor Compensation," in *2020 55th International Universities Power Engineering Conference (UPEC)*, Turin, Italy, Sep. 2020, pp. 1–6, <https://doi.org/10.1109/UPEC49904.2020.9209786>.
- [7] L. M. Escibano, R. Prieto, J. A. Oliver, J. A. Cobos, and J. Uceda, "New modeling strategy for the fringing energy in magnetic components with air gap," in *APEC. Seventeenth Annual IEEE Applied Power Electronics Conference and Exposition (Cat. No.02CH37335)*, Dallas,

TX, USA, Mar. 2002, vol. 1, pp. 144–150 vol.1, <https://doi.org/10.1109/APEC.2002.989240>.

- [8] S. Grebovic, N. Oprasic, and A. Balota, "Influence of Shunt Reactor Switching on Overvoltages in 400 kV Substation," in *2020 9th Mediterranean Conference on Embedded Computing (MECO)*, Budva, Montenegro, Jun. 2020, pp. 1–4, <https://doi.org/10.1109/MECO49872.2020.9134116>.
- [9] R. P. Hutahaean and G. Sianipar, "Transient analysis of 150 kV shunt reactor at Bulukumba Substation," in *Proceedings of the 2011 International Conference on Electrical Engineering and Informatics*, Bandung, Indonesia, Jul. 2011, pp. 1–6, <https://doi.org/10.1109/ICEEL2011.6021818>.
- [10] H. B. Duc, T. P. Minh, T. P. Anh, and V. D. Quoc, "A Novel Approach for the Modeling of Electromagnetic Forces in Air-Gap Shunt Reactors," *Engineering, Technology & Applied Science Research*, vol. 12, no. 1, pp. 8223–8227, Feb. 2022, <https://doi.org/10.48084/etasr.4692>.
- [11] V. D. Quoc, "Robust Correction Procedure for Accurate Thin Shell Models via a Perturbation Technique," *Engineering, Technology & Applied Science Research*, vol. 10, no. 3, pp. 5832–5836, Jun. 2020, <https://doi.org/10.48084/etasr.3615>.
- [12] V. D. Quoc, "Accurate Magnetic Shell Approximations with Magnetostatic Finite Element Formulations by a Subdomain Approach," *Engineering, Technology & Applied Science Research*, vol. 10, no. 4, pp. 5953–5957, Aug. 2020, <https://doi.org/10.48084/etasr.3678>.
- [13] R. V. Sabariego, "The Fast Multipole Method for electromagnetic field computation," Ph.D. dissertation, University of Vigo, Vigo, Spain, 2004.
- [14] R. L. Burden, J. D. Faires, and A. M. Burden, *Numerical Analysis*. Boston, MA, USA: Cengage Learning, 2015.